Activated Platelets Interfere with Recruitment of Mesenchymal Stem Cells to Apoptotic Cardiac Cells via High Mobility Group Box 1/Toll-like Receptor 4-mediated Down-regulation of Hepatocyte Growth Factor Receptor MET*

Sebastian Vogel[‡], Madhumita Chatterjee[‡], Katja Metzger[‡], Oliver Borst[‡], Tobias Geisler[‡], Peter Seizer[‡], Iris Müller[‡], Andreas Mack[§], Susanne Schumann[¶], Hans-Jörg Bühring[¶], Florian Lang[∥], Rüdiger V. Sorg**, Harald Langer[‡], and Meinrad Gawaz[‡1]

From the ‡Department of Cardiology and Cardiovascular Diseases, the §Institute of Anatomy, the ¶Department of Oncology, Haematology, Immunology, Rheumatology and Pulmonology, and the ∥Institute of Physiology, Eberhard Karls University, 72076 Tübingen, Germany and the **Institute for Transplantation Diagnostics and Cell Therapeutics, Heinrich Heine University of Düsseldorf, 40225 Düsseldorf, Germany

Background: Mesenchymal stem cells (MSC) contribute to cardiac repair after myocardial injury. Underlying molecular mechanisms remain unexplored.

Results: Activated platelets inhibit recruitment of MSC to apoptotic cardiac myocytes and fibroblasts via HMGB1/TLR-4-mediated down-regulation of HGF receptor MET.

Conclusion: We identify a novel mechanism by which platelets impair MSC migration to damaged cardiac cells.

Significance: The cross-talk between platelets and MSC might be critical for myocardial repair.

Recruitment of mesenchymal stem cells (MSC) following cardiac injury, such as myocardial infarction, plays a critical role in tissue repair and may contribute to myocardial recovery. However, the mechanisms that regulate migration of MSC to the site of tissue damage remain elusive. Here, we demonstrate *in vitro* that activated platelets substantially inhibit recruitment of MSC toward apoptotic cardiac myocytes and fibroblasts. The alarmin high mobility group box 1 (HMGB1) was released by platelets upon activation and mediated inhibition of the cell death-dependent migratory response through Toll-like receptor (TLR)-4 expressed on the MSC. Migration of MSC to apoptotic cardiac myocytes and fibroblasts was driven by hepatocyte growth factor (HGF), and platelet activation was followed by HMGB1/TLR-4-dependent down-regulation of HGF receptor MET on MSC, thereby impairing HGF-driven MSC recruitment. We identify a novel mechanism by which platelets, upon activation, interfere with MSC recruitment to apoptotic cardiac cells, a process that may be of particular relevance for myocardial repair and regeneration.

Cardiac repair and regeneration following ischemic injury as seen with myocardial infarction is typically associated with an inflammatory reaction that leads to a well orchestrated healing process, collagen deposition, and the formation of scar tissue (1,

2). However, postinfarction ventricular remodeling is known to result in infarct expansion and progressive ventricular dilation, which is associated with adverse clinical outcomes (3).

Mesenchymal stem cells (MSC),[2] multipotent non-hematopoietic stem cells that typically originate from the bone marrow (4–5), have been suggested to play a critical role in repair and regeneration of the injured myocardium (6, 7). Besides their capability of differentiating into cardiac myocytes (8) and fibroblasts (9), which are the main cellular constituents of the heart, they exert antiapoptotic and antifibrotic effects that may prevent cardiac remodeling (10, 11). Such paracrine activities make them promising therapeutic vehicles in cardiac repair (12–13). After myocardial infarction and intramyocardial (14), intracoronary (15), or intravenous (16) transplantation of MSC, the cells have been shown to infiltrate the injured heart and significantly restore cardiac function. Moreover, various clinical studies could confirm beneficial effects of MSC after myocardial damage (17, 18). However, the clinical benefit has been discussed controversially, and the success of MSC-based therapy for myocardial infarction has been limited due to its often short lived efficacy (7). Therefore, a better understanding of the underlying molecular mechanisms that control MSC recruitment to the damaged myocardium is necessary to improve efficacy of treatment.

Recently, we could demonstrate that apoptotic but not necrotic cardiomyocytes produce hepatocyte growth factor (HGF) and induce recruitment of MSC via HGF receptor MET, providing a link between apoptotic cell death and the attraction

[2] The abbreviations used are: MSC, mesenchymal stem cell(s); HMGB1, high mobility group box 1; TLR, Toll-like receptor; HGF, hepatocyte growth factor; RAGE, receptor of advanced glycation end products; PI, propidium iodide; CM, conditioned medium; PRP, platelet-rich plasma; CRP, C-reactive protein.

of MSC (19). HGF is a growth factor known to be produced after myocardial ischemia, as investigated in animals (20) and humans (21). With its antiapoptotic (22), proangiogenic (23), and immunosuppressive (24) activity, it confers cardioprotection (25), implying that HGF-mediated recruitment of MSC to apoptotic cardiomyocytes may exert tissue-protective effects after myocardial injury.

Platelets, as the dominant and first cells that accumulate at sites of disrupted vascular and tissue integrity, are capable of regulating these cell death-dependent tissue repair mechanisms (26). Platelets are well known to play a key role in coronary thrombosis and acute myocardial infarction (27–31). Upon activation, they release a multitude of biologically active mediators, such as cytokines, chemokines, and growth factors, into their microenvironment that regulate recruitment, adhesion, and proliferation of adult stem cells, including MSC (26). Moreover, platelets cytoplasmically express high mobility group box 1 (HMGB1), a protein typically expressed in the nucleus of almost all mammalian cells that acts as a danger signal and activates immune responses when released into the extracellular matrix during cellular stress responses (32–34). Upon platelet activation, HMGB1 has been described to be exported to the cell surface (34). In patients with acute myocardial infarction, serum levels of HMGB1 were significantly increased, peaking 12 h after infarction (35). Elevated levels were associated with adverse clinical outcomes, including pump failure, cardiac rupture, and in-hospital cardiac deaths. However, in experimental models of myocardial infarction, detrimental as well as cardioprotective effects of HMGB1 have been reported (36–38). HMGB1 activates pattern recognition receptors Toll-like receptor (TLR)-4, TLR-2, and the receptor of advanced glycation end products (RAGE), a transmembrane multiligand receptor of the immunoglobulin superfamily (39, 40). MSC have been reported to express these receptors for HMGB1 (41, 42), implying that MSC might be a putative target of platelet-derived HMGB1 in the process of MSC recruitment to injured cardiac cells.

In this study, we show *in vitro* that platelets substantially inhibit recruitment of MSC to apoptotic cardiac myocytes and fibroblasts. Once activated, platelets release the alarmin HMGB1, which mediates inhibition of the cell death-dependent migratory response via TLR-4 expressed on the MSC. HGF drives MSC migration to apoptotic cardiac cells, and HGF receptor MET is down-regulated on MSC as a consequence of TLR-4 engagement by platelet-derived HMGB1, thereby inhibiting MSC recruitment. We provide evidence for the first time that platelet activation impairs MSC migration to apoptotic cardiac cells and identify the molecular mechanism that mediates this platelet/MSC interaction.

EXPERIMENTAL PROCEDURES

Mesenchymal Stem Cells—Human bone marrow was obtained from volunteer donors after informed consent (as approved by the local ethical committee). MSC were isolated from bone marrow as described previously (19). In brief, mononuclear cells were obtained by Ficoll (Biochrom, Berlin, Germany) gradient centrifugation and ammonium chloride lysis of residual red blood cells. Mononuclear cells were plated in

75-cm^2 cell culture flasks (Costar/Corning) in DMEM (Lonza, Verviers, Belgium) supplemented with 30% fetal calf serum (FCS; Invitrogen), 100 units/ml penicillin, 100 μg/ml streptomycin, and 2 mM L-glutamine (all from Lonza). After 48 h of cell culture at 37 °C and 5% CO_2, non-adherent cells were removed. When reaching 80% confluence, cells were harvested with trypsin (Lonza) and replated at 1:3. Only cells from passages 3–8 were used for experiments. Immunophenotyping was performed as described before (19). All MSC preparations showed the typical (4) immunophenotype (positive for CD29, CD73, CD90, and CD105; negative for CD11b, CD34, and CD45) and osteogenic and adipogenic differentiation potential (data not shown).

Cardiac Myocytes and Cardiac Fibroblasts—Human cardiac myocytes and human cardiac fibroblasts, both isolated primary cells from the ventricles of an adult heart, were obtained from Promo Cell (Heidelberg, Germany), cultured in myocyte growth medium or fibroblast growth medium 3 (both from PromoCell) according to the manufacturer's instructions, and incubated at 37 °C and 5% CO_2 in a humidified atmosphere. To confirm their identity as cardiac myocytes or fibroblasts, immunofluorescence stainings with a monoclonal antibody against sarcomeric α-actinin (1 μg/ml; mouse IgG1; Abcam, Cambridge, MA) and a polyclonal antibody against fibroblast-specific protein 1 (S100A4; 2 μg/ml; goat IgG; Biorbyt, Cambridge, UK) were carried out. For this, the cells were grown for 24 h on coverslips kept within a 24-well culture plate in their respective culture media. Subsequently, cells were fixed with 2% paraformaldehyde, permeabilized with 0.5% Triton X-100, and blocked with 1% BSA-PBS for 1 h. Cells were incubated overnight at 4 °C with the respective primary antibodies, washed with PBS + 0.3% Triton X-100 + 0.1% Tween 20, and incubated with Alexa Fluor 488-tagged goat anti-mouse IgG or donkey anti-goat IgG (both 1:100; Invitrogen) for 2 h at room temperature. Following another washing step, nuclei were stained by incubation with TO-PRO-3 iodide for 15 min (final 1 μM; Molecular Probes, Inc., Eugene, OR). Cells were washed again, and coverslips were mounted with antifade fluorescence mounting medium (Dako, Hamburg, Germany). Confocal immunofluorescence analysis was performed using a LSM510 META confocal laser-scanning microscope and ZEN 2012 imaging software (Carl Zeiss).

Induction and Detection of Apoptosis and Necrosis in Cardiac Myocytes and Cardiac Fibroblasts—Induction of apoptosis in cardiac myocytes and fibroblasts was carried out by incubation with 300 nM staurosporine (Calbiochem) or 10 mM sodium azide (Sigma-Aldrich) for 3 h. Necrosis was initiated by treatment with 40 μM H_2O_2 (Sigma-Aldrich) for 3 h or 25% ethanol (Sigma-Aldrich) for 1 h (19). Apoptotic and necrotic cell death of cardiac myocytes and fibroblasts was confirmed with annexin V/propidium iodide (PI) staining and flow cytometry as recommended by the manufacturer (Beckman-Coulter, Krefeld, Germany), using a FACSCalibur flow cytometer with CellQuest software (BD Biosciences). After induction of apoptosis or necrosis, culture medium was exchanged, and cells were incubated for 12 h to obtain conditioned medium (CM).

Isolation and Activation of Platelets—Human platelets were isolated as described before (43). In brief, venous blood was

drawn from the antecubital vein of healthy volunteers and collected in acid-citrate-dextrose buffer. Blood was centrifuged at $430 \times g$ for 20 min, platelet-rich plasma (PRP) was added to Tyrode's-HEPES buffer (HEPES (2.5 mmol/liter), NaCl (150 mmol/liter), KCl (1 mmol/liter), $NaHCO_3$ (2.5 mmol/liter), NaH_2PO_4 (0.36 mmol/liter), glucose (5.5 mmol/liter), BSA (1 mg/ml), pH 6.5) and centrifuged at $900 \times g$ for 10 min. The supernatant was discarded, and the platelet pellet was suspended in Tyrode's-HEPES buffer (pH 7.4; supplemented with $CaCl_2$ (1 mmol/liter), $MgCl_2$ (1 mmol/liter)). For certain experiments, 3×10^8 freshly isolated platelets were activated in 1 ml of PBS (pH 7.4; Lonza) by treatment with 50 μM ADP (Chrono-Log, Havertown, PA) or 5 μg/ml C-reactive protein (CRP; from Richard Farndale, University of Cambridge) for 5, 15, or 30 min and centrifuged at $900 \times g$ for 5 min to obtain platelet supernatant. Generation of platelet supernatant from unactivated (resting) platelets followed the same procedure in the absence of platelet agonists.

Cell Migration Assay—Migration of MSC toward vital, apoptotic, or necrotic cardiac myocytes or cardiac fibroblasts was analyzed in 24-well plates and transwell cell culture inserts with 8-μm pore membrane filters (Costar/Corning). MSC (10^5 cells/well in 200 μl of DMEM supplemented with 0.5% BSA) were loaded into the upper chamber, and CM derived from vital, apoptotic, or necrotic cardiac myocytes or fibroblasts or recombinant HGF (20–60 ng/ml; R&D Systems, Wiesbaden, Germany) served as chemoattractants that were loaded into the bottom chamber. When indicated, MSC were preincubated in 24-well plates for 24 h with platelet supernatants supplemented with 10% FCS (CM derived from platelets; 2×10^5 cells/well in 300 μl) or with PBS supplemented with 10% FCS containing ADP (50 μM) or CRP (5 μg/ml) or with recombinant HMGB1 (10–40 ng/ml; R&D Systems). Further, neutralization studies were performed by adding neutralizing anti-HMGB1 antibody (10 μg/ml, mouse IgG2b κ; Biolegend, San Diego, CA), irrelevant isotype control antibody (10 μg/ml, mouse IgG2b κ; Biolegend), or glycyrrhizin, a specific HMGB1 inhibitor (10 μg/ml; Calbiochem), to CM derived from activated platelets prior to preincubation of the MSC. In other experiments, HMGB1-receptors RAGE, TLR-2, and TLR-4 were blocked on MSC prior to MSC preincubation with CM of activated platelets or recombinant HMGB1 by treatment with anti-human RAGE polyclonal antibody (20 μg/ml, goat IgG), anti-human TLR-2 monoclonal antibody (2 μg/ml, mouse IgG2b), or anti-human TLR-4 polyclonal antibody (10 μg/ml, goat IgG) (all from R&D Systems). To study the contribution of HGF to MSC migration toward apoptotic cardiac myocytes or fibroblasts, neutralizing anti-HGF polyclonal antibody (1 μg/ml, goat IgG; R&D Systems) or normal goat IgG (1 μg/ml; Santa Cruz Biotechnology, Inc.) was added to the targets in the bottom chambers of the transwell system.

To evaluate migration of MSC, the plates were incubated at 37 °C and 5% CO_2 for 12 h, the upper side of the filters was then carefully washed with PBS, and remaining cells that had not penetrated the filters were removed with cotton swabs. Cells that had migrated to the lower surface of the filters were fixed in methanol and then stained with hematoxylin (Merck). After being washed, migrated cells were observed with a light microscope at $\times 10$ magnification, pictures were captured, and migrated cells were counted in the center of each filter.

Assessment of HMGB1 Release upon Platelet Activation—To determine the distribution of HMGB1 in resting and activated platelets, isolated platelets (3×10^8 cells/ml) were incubated with 50 μM ADP, 5 μg/ml CRP or PBS for 15 min and fixed with 1% paraformaldehyde. Subsequently, platelets were applied to 0.01% poly-L-lysine-coated coverslips and permeabilized with 0.3% Triton X-100. After blocking with 1% BSA-PBS for 1 h, cells were incubated overnight at 4 °C with anti-HMGB1 polyclonal antibody (2 μg/ml; rabbit IgG; Sigma-Aldrich). After washing with PBS + 0.3% Triton X-100 + 0.1% Tween 20, platelets were incubated with Alexa Fluor 488-tagged goat anti-rabbit IgG (1:100; Invitrogen) for 2 h at room temperature and washed, and the coverslips were mounted with antifade fluorescence mounting medium. Confocal immunofluorescence analysis was carried out as described above.

To investigate the effect of platelet activation on HMGB1 release, Western blot analysis was performed. Isolated platelets (3×10^8 cells/ml) were incubated with 5 μg/ml CRP or PBS for 5, 15, or 30 min and centrifuged at $900 \times g$ for 5 min. Platelet supernatants were removed and supplemented with protease inhibitor mixture (Sigma-Aldrich). Corresponding cell pellets were lysed in lysis buffer (Tris, pH 7.4 (50 mM), NaCl (150 mM), Triton X-100 (1%), Na_2HPO_4 (0.5%), mercaptoethanol (0.4%)) containing protease inhibitor mixture for 60 min at 4 °C. Protein concentrations in platelet lysates as well as supernatants were determined with a Bradford protein assay (Bio-Rad), and 50 μg (lysate) or 20 μg (supernatant) of proteins were resolved by 8.5% SDS-PAGE. Immunoblotting onto PVDF membranes (Immobilon P, Millipore, Billerica, MA) was performed using the Semi-Dry Transfer Cell System (Peqlab, Erlangen, Germany). Membranes were incubated overnight at 4 °C with anti-HMGB1 polyclonal antibody (2 μg/ml; rabbit IgG; Sigma-Aldrich), and anti-actin polyclonal antibody (1:1000; rabbit IgG; Abcam) was used as an internal loading control. For detection of antibody binding, corresponding secondary fluorescence-labeled antibodies and the Odyssey infrared imaging system (LI-COR, Bad Homburg, Germany) were used. Bands were quantified by ImageJ software (National Institutes of Health, Bethesda, MD).

HMGB1 release upon platelet activation was further investigated by ELISA. Isolated platelets (3×10^8 cells/ml) were incubated with 50 μM ADP, 5 μg/ml CRP or PBS for 5, 15, or 30 min and centrifuged at $900 \times g$ for 5 min. HMGB1 levels in platelet supernatants were determined using HMGB1-ELISA (Shino Test Corp., Kanagawa, Japan) following the manufacturer's protocol. To evaluate the extent of platelet activation, platelets were incubated with 50 μM ADP, 5 μg/ml CRP or PBS for 5, 15, or 30 min, and surface expression of P-selectin (CD62P) was investigated by flow cytometry as described previously (44) using fluorescein isothiocyanate (FITC)-conjugated monoclonal anti-CD62P antibody (mouse IgG1; Beckman Coulter, Krefeld, Germany).

Flow Cytometric Detection of HMGB1 Receptor Expression on MSC—Expression of the HMGB1 receptors RAGE, TLR-2, and TLR-4 on MSC was evaluated by flow cytometry using anti-human RAGE monoclonal antibody (mouse IgG2a; Abcam),

anti-human TLR-2 monoclonal antibody (mouse IgG2b; R&D Systems), and anti-human TLR-4 polyclonal antibody (goat IgG; R&D Systems). Phycoerythrin-conjugated F(ab′)2 goat anti-mouse IgG and F(ab′)2 donkey anti-goat IgG (both from Santa Cruz Biotechnology) were used as secondary antibodies. Cells were analyzed on a FACSCalibur flow cytometer with CellQuest software.

Small Interfering RNA Transfection—TLR-4 small interfering RNA (siRNA) (ON-TARGET plus Human TLR4 siRNA SMART pool; Thermo Scientific) was used to knock down TLR-4 expression in MSC. A non-targeting sequence (ON-TARGET Plus Non-targeting Control Pool; Thermo Scientific) served as a control. siRNA was mixed with Lipofectamine transfection reagent (Lipofectamine RNAiMAX; Invitrogen) in serum-free medium (Opti-MEM; Invitrogen) according to the manufacturer's instructions. Subsequently, MSC growing in 6-well plates at a confluence of 70% were transfected with siRNA (10 nM) in culture medium, and cells were cultivated at 37 °C for 48 h. At the end of the culture period, cells were washed with PBS and lysed in cell lysis buffer for Western blot analysis as described above. Expression of TLR-4 was detected with anti-TLR4 polyclonal antibody (1 μg/ml; rabbit IgG; Santa Cruz Biotechnology), and anti-actin polyclonal antibody (1:1000; rabbit IgG; Abcam) was used as an internal loading control. To evaluate migratory potential of the transfected MSC, cells were harvested, preincubated with CM derived from activated platelets, and used in migration assays with CM of apoptotic cardiac myocytes or fibroblasts as targets.

Immunofluorescence Staining of Intracellular HGF in Vital, Apoptotic, and Necrotic Cardiac Myocytes—Cardiac myocytes were grown for 24 h on coverslips kept within a 24-well culture plate in myocyte growth medium prior to induction of apoptosis (staurosporine, 300 nM, 3 h) or necrosis (H_2O_2, 40 μM, 3 h). For immunofluorescence staining of intracellular HGF, vital (untreated), apoptotic, and necrotic cardiac myocytes were subsequently fixed, permeabilized, and blocked as described above. Cells were incubated overnight at 4 °C with anti-HGF (C-terminal) polyclonal antibody (5 μg/ml; rabbit Ig; Abgent, San Diego, CA), washed with PBS + 0.3% Triton X-100 + 0.1% Tween 20, and incubated with Alexa Fluor 488-tagged goat anti-rabbit IgG (1:100) for 2 h at room temperature. Staining of nuclei was carried out with TO-PRO-3 iodide, and cells were mounted with antifade fluorescence mounting medium. Confocal microscopic analysis was subsequently performed as described above.

HGF ELISA—HGF levels in CM derived from vital cardiac myocytes and fibroblasts or harvested 12 h after induction of apoptosis or necrosis (see above) were determined using an ELISA kit (Gentaur, Brussels, Belgium).

Assessment of HGF Receptor MET Expression on MSC—MSC were grown for 24 h on coverslips in 24-well plates in culture medium and subsequently incubated for a further 24 h with supernatant of ADP- or CRP-activated platelets supplemented with 10% FCS (CM) or in PBS supplemented with 10% FCS. Cells were fixed with 2% paraformaldehyde, blocked with 1% BSA-PBS for 1 h, incubated overnight at 4 °C with anti-human MET polyclonal antibody (1:500 dilution; rabbit IgG; Abcam), washed with PBS + 0.1% Tween 20, and incubated with Alexa

Fluor 488-tagged goat anti-rabbit IgG (1:100) for 2 h at room temperature. Following another washing step, nuclei were stained by incubation with TO-PRO-3 iodide, coverslips were mounted with antifade fluorescence mounting medium, and confocal microscopic analysis was performed as described above. ZEN 2012 imaging software was used to quantify mean fluorescence intensities.

Expression of MET on MSC was also determined by flow cytometry. MSC were incubated with supernatant of ADP- or CRP-activated platelets supplemented with 10% FCS (CM) or in PBS supplemented with 10% FCS in 24-well plates. After 2, 4, 12, and 24 h of incubation, MSC were detached with a cell scraper and labeled with fluorescein-conjugated anti-human MET monoclonal antibody (10 μg/ml; clone 95106, mouse IgG1; R&D Systems). Expression of MET was detected and quantified by mean fluorescence intensity in flow cytometry.

To further study MET expression on MSC, cells were cultured for 12 h in the presence or absence of CM derived from CRP- or ADP-activated platelets and subsequently fractionated into plasma membrane and cytosolic components using a plasma membrane protein extraction kit (Abcam) according to the manufacturer's protocol. The distinct fractions were separated by SDS-PAGE and transferred to PVDF membranes for Western blot analysis using anti-MET monoclonal antibody (1:500; mouse IgG1; Cell Signaling) and anti-actin polyclonal antibody (1:1000; rabbit IgG; Abcam) as an internal loading control. Bands were visualized and quantified as described above.

Statistical Analysis—All data are presented as mean $\pm$ S.E. for $n \geq 3$ unless stated otherwise. Statistical significance was determined with Student's t test using GraphPad Prism software (GraphPad, San Diego, CA).

RESULTS

MSC Migrate toward Apoptotic but Not Necrotic or Vital Cardiac Myocytes and Fibroblasts—Prior to induction of apoptosis and necrosis in human cardiac myocytes and fibroblasts, the identity of the cells was confirmed by intracellular detection of sarcomeric α-actinin and fibroblast-specific protein 1 (S100A4) with immunofluorescence staining and confocal laser-scanning microscopy (Fig. 1*A*). Apoptosis was induced by staurosporine or sodium azide, and necrosis was induced by H_2O_2 or ethanol. The extent of apoptosis and necrosis in cardiac myocytes and fibroblasts was determined after 12 h using annexin V/PI double staining and flow cytometry (staurosporine and sodium azide, 43.9–58.3% annexin V^+/PI^- early apoptotic cells and 8.4–13.2% annexin V^+/PI^+ secondary necrotic cells; H_2O_2 and ethanol, 71.3–89.5% annexin V^-/PI^+ necrotic cells; Fig. 1*B*). To evaluate the migratory response of MSC toward vital, apoptotic, and necrotic cardiac myocytes and fibroblasts, transwell migration experiments were performed (Fig. 1*C*). CM derived from apoptotic but not necrotic or vital cardiac cells induced migration of MSC.

Activated Platelets Inhibit Migration of MSC to Apoptotic Cardiac Myocytes and Fibroblasts—To investigate whether platelets have an influence on recruitment of MSC to apoptotic cardiac myocytes and fibroblasts, MSC were preincubated with CM derived from activated (CRP- or ADP-treated) or non-ac-
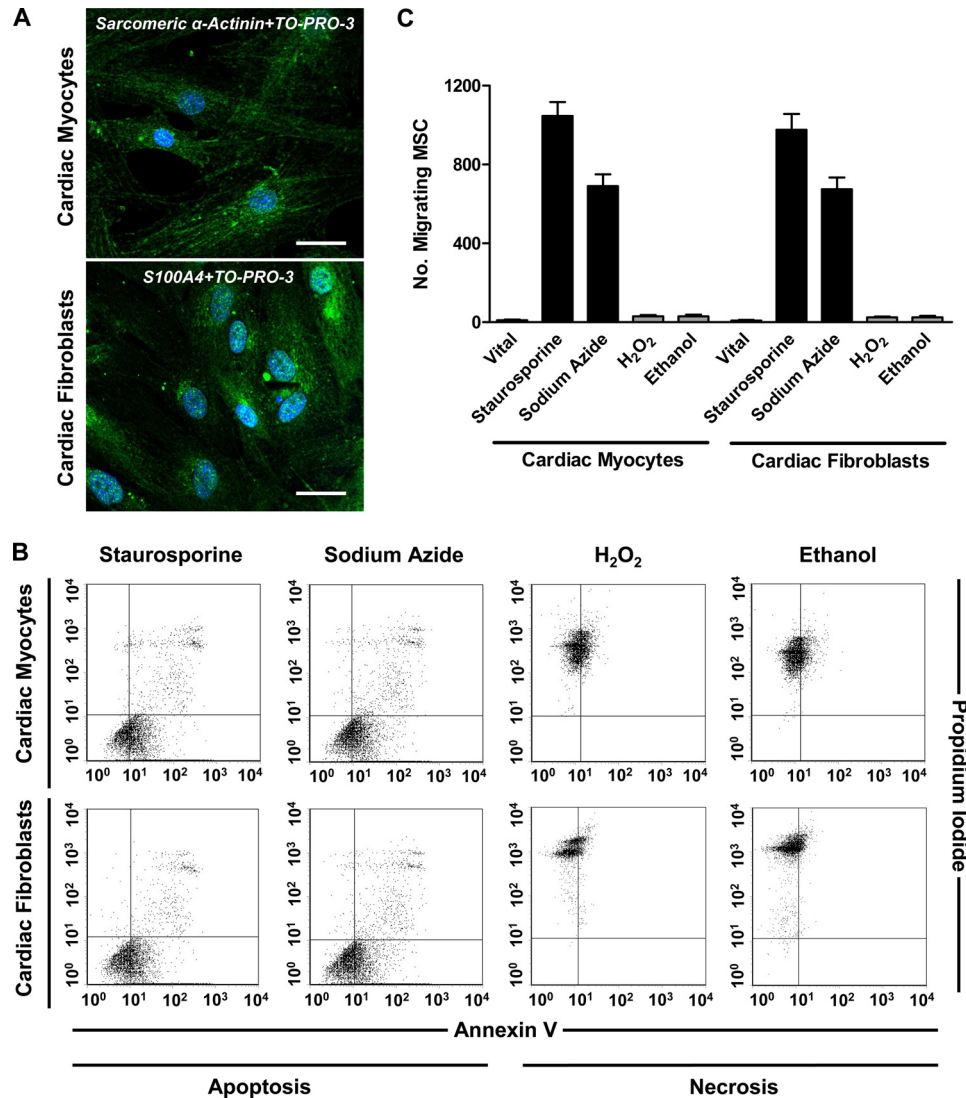
FIGURE 1. **Induction and detection of apoptosis and necrosis in cardiac myocytes and cardiac fibroblasts and chemoattractive activity for MSC.** *A*, expression of sarcomeric α-actinin in cardiac myocytes and S100A4 in cardiac fibroblasts was determined by immunofluorescence staining and confocal laser-scanning microscopy. *Scale bar*, 30 μm. *B*, induction of apoptosis (300 nM staurosporine, 3 h; 10 mM sodium azide, 3 h) and necrosis (40 μM H$_2$O$_2$, 3 h; 25% ethanol, 1 h) in cardiac myocytes and fibroblasts was confirmed by flow cytometric evaluation of the frequencies of apoptotic (annexin V$^+$/PI$^-$), necrotic (annexin V$^-$/PI$^+$), and secondary necrotic (annexin V$^+$/PI$^+$) cells. Quadrants were set according to isotype controls or to untreated cells. *C*, migration of MSC toward conditioned media derived from vital (untreated), apoptotic, or necrotic cardiac myocytes and fibroblasts was assessed in a transwell migration assay. The number of migrating cells was determined after 12 h. Data are presented as mean $\pm$ S.E. (*error bars*) ($n \geq 3$).

tivated (resting) isolated platelets for 24 h prior to evaluating migration. Incubation of the MSC with CRP or ADP alone served as controls. Remarkably, CM of CRP-activated as well as ADP-activated platelets strongly inhibited recruitment of MSC toward CM derived from apoptotic cardiac myocytes (staurosporine, 55.9 $\pm$ 7.4/48.0 $\pm$ 6.8% inhibition; $p < 0.004$ (Fig. 2*A*); sodium azide, 49.0 $\pm$ 11.0/47.1 $\pm$ 8.8% inhibition; $p < 0.011$ (Fig. 2*B*)) and apoptotic cardiac fibroblasts (staurosporine, 57.4 $\pm$ 9.1/49.2 $\pm$ 9.5% inhibition; $p < 0.008$ (Fig. 2*C*); sodium azide, 53.0 $\pm$ 8.9/49.4 $\pm$ 7.6% inhibition; $p < 0.008$ (Fig. 2*D*)). In contrast, neither CM derived from resting platelets nor CRP or ADP in the absence of platelets had any influence on MSC migration to the apoptotic targets.

Platelet Activation Results in Release of HMGB1—To analyze the molecular mechanism underlying platelet-mediated inhibition of MSC recruitment to apoptotic cardiac cells, we deter-

mined the presence of one candidate factor, HMGB1, in platelets and CM derived from platelets. Fig. 3*A* shows representative immunofluorescence confocal laser-scanning microscopy images of permeabilized non-activated (resting) and activated (treated with CRP or ADP) platelets stained with an HMGB1-specific antibody. HMGB1 was present in the cytosol of resting platelets, whereas it became translocated toward the plasma membrane upon activation with CRP or ADP. Moreover, Western blot analysis performed on platelet lysates as well as supernatants revealed strong HMGB1 expression in resting platelets (lysate) and, upon activation with CRP, a time-dependent and significant decrease of HMGB1 protein abundance in lysates ($p < 0.04$) and increase in the respective supernatants ($p < 0.01$), indicating an HMGB1 release phenomenon (Fig. 3*B*). To further substantiate release of HMGB1 by activated platelets, we analyzed CM derived from isolated platelets
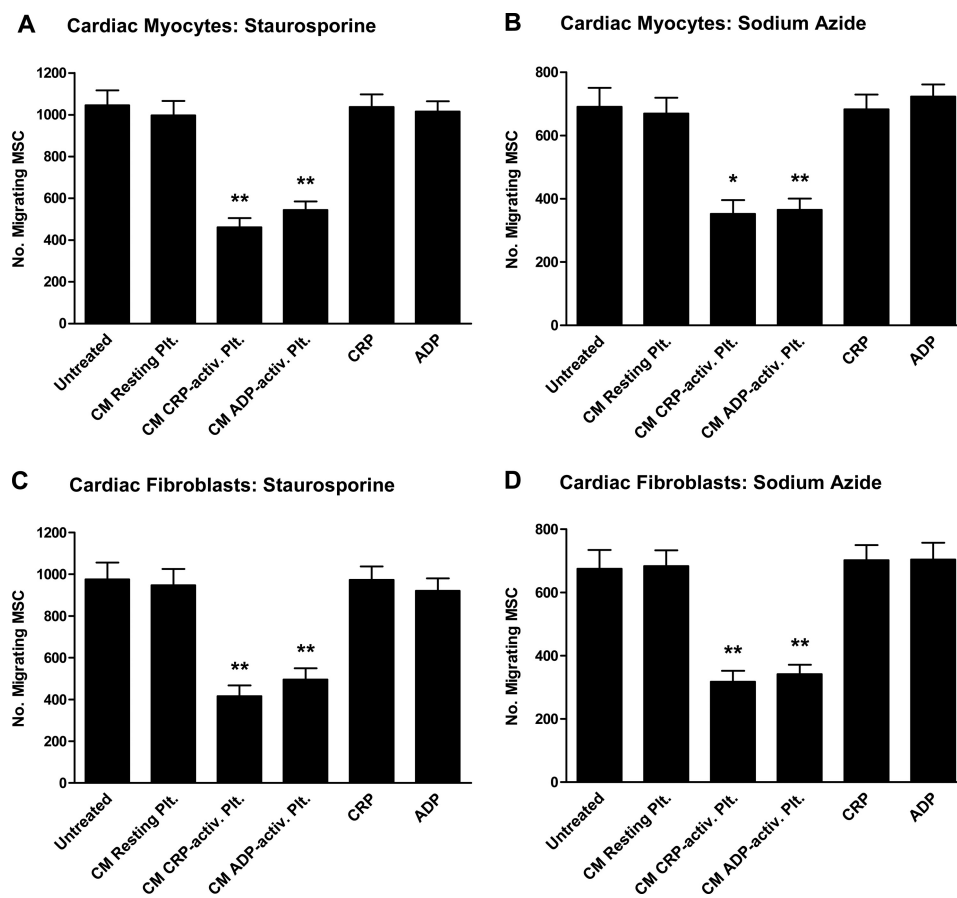
FIGURE 2. **Influence of resting and activated platelets on MSC migration to apoptotic cardiac myocytes and fibroblasts.** Conditioned media derived from staurosporine-treated (*A* and *C*) or sodium azide-treated (*B* and *D*) cardiac myocytes (*A* and *B*) or cardiac fibroblasts (*C* and *D*) served as chemoattractants for MSC in a transwell migration assay. In certain experiments, MSC were preincubated with conditioned media derived from resting (untreated) or activated (5 μg/ml CRP, 30 min; 50 μM ADP, 30 min) platelets for 24 h prior to evaluating migration. 24-h incubation of the MSC with CRP (5 μg/ml) or ADP (50 μM) in the absence of platelets served as controls. The number of migrating MSC was determined after 12 h. Data are presented as mean $\pm$ S.E. (*error bars*) for $n \geq 3$. Statistical significance for the comparison with untreated MSC is indicated (*, $p < 0.02$; **, $p < 0.01$).

(resting and activated with ADP or CRP) for the presence of HMGB1 using ELISA (Fig. 3*C*). Indeed, significant amounts of HMGB1 were detected only in CM derived from activated platelets. Moreover, HMGB1 levels in CM increased depending on the duration of platelet activation and corresponded to an enhanced surface expression of CD62P (P-selectin) denoting platelet activation as evaluated by flow cytometry.

Activated Platelets Inhibit MSC Recruitment to Apoptotic Cardiac Myocytes and Fibroblasts through HMGB1/TLR-4— Having detected release of HMGB1 associated with platelet activation, we investigated the potential role of HMGB1 in platelet-mediated inhibition of the cell death-dependent MSC recruitment. The addition of a neutralizing anti-HMGB1 antibody to CM derived from CRP-activated platelets prior to MSC preincubation strongly reversed the inhibitory effect of activated platelets on MSC recruitment toward CM of apoptotic cardiac myocytes (staurosporine, 55.9 $\pm$ 7.4 *versus* 16.3 $\pm$ 7.3% inhibition ($p < 0.003$); sodium azide, 49.0 $\pm$ 11.0 *versus* 15.8 $\pm$ 9.6% inhibition ($p < 0.018$); Fig. 4*A*) and apoptotic cardiac fibroblasts (staurosporine, 57.4 $\pm$ 9.1 *versus* 14.8 $\pm$ 10.1% inhibition ($p < 0.006$); sodium azide, 53.0 $\pm$ 8.9 *versus* 16.2 $\pm$ 9.9% inhibition ($p < 0.009$); Fig. 4*C*). Neutralizing HMGB1 bioactivity in CM derived from ADP-activated platelets was followed by similar effects on MSC migration toward CM of apoptotic car-

diac myocytes (staurosporine, 48.0 $\pm$ 6.8 *versus* 14.8 $\pm$ 6.5% inhibition ($p < 0.004$); sodium azide, 47.1 $\pm$ 8.8 *versus* 13.5 $\pm$ 8.5% inhibition ($p \leq 0.009$); Fig. 4*B*) and apoptotic cardiac fibroblasts (staurosporine, 49.2 $\pm$ 9.5 *versus* 13.7 $\pm$ 8.3% inhibition ($p < 0.009$); sodium azide, 49.4 $\pm$ 7.6 *versus* 13.0 $\pm$ 8.3% inhibition ($p < 0.006$); Fig. 4*D*). Comparable results were also obtained when glycyrrhizin, a specific HMGB1 inhibitor, was used (Fig. 4, *A–D*). An irrelevant isotype-matched control Ig antibody had no effect on platelet-mediated inhibition of MSC migration.

To define the receptor that mediates the observed platelet HMGB1-driven inhibitory effect on MSC migration, we determined surface expression of the well known HMGB1 receptors RAGE, TLR-2, and TLR-4 on MSC by flow cytometry (Fig. 5*A*). MSC were positive for RAGE and TLR-4 and negative for TLR-2. Next, MSC were treated with neutralizing antibodies to RAGE, TLR-2, and TLR-4 to block the respective HMGB1 receptors, thereafter incubated with CM derived from activated platelets, and then tested for their migration toward apoptotic cardiac myocytes (Fig. 5, *B* and *C*) and apoptotic cardiac fibroblasts (Fig. 5, *D* and *E*). Only blocking TLR-4 on MSC could reverse the inhibitory effect of CM derived from CRP-activated platelets on MSC migration toward CM of apoptotic cardiac myocytes (staurosporine, 55.9 $\pm$ 7.4 *versus* 8.2 $\pm$ 7.0% inhibi-
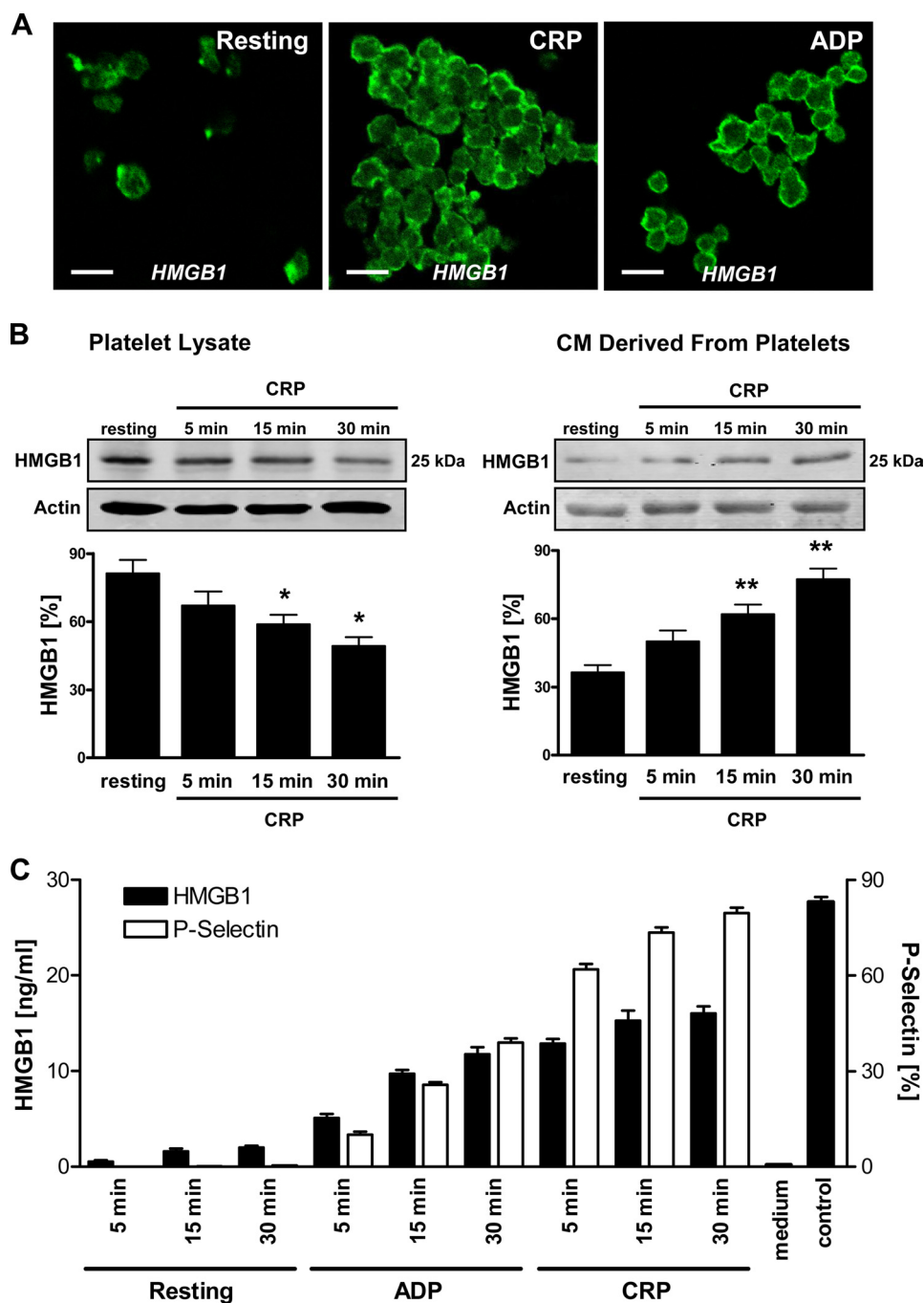
FIGURE 3. **Expression of HMGB1 in platelets and release upon platelet activation.** *A*, expression of intracellular HMGB1 in resting (untreated) and activated (5 μg/ml CRP, 15 min; 50 μM ADP, 15 min) platelets was determined by immunofluorescence staining and confocal laser-scanning microscopy. An HMGB1-specific polyclonal antibody and an Alexa Fluor 488-tagged antibody (*green*) were used. Representative images of three independent experiments. *Scale bar*, 5 μm. *B*, HMGB1 protein levels in lysates and conditioned media derived from resting and CRP-activated platelets (5 μg/ml CRP; 5, 15, and 30 min) were deciphered by Western blot analysis, detecting HMGB1 at 25 kDa. An actin polyclonal antibody served as loading control. Statistical significance (*, $p < 0.04$; **, $p < 0.01$) of densitometric analysis of HMGB1 bands (normalized to actin) is indicated. *C*, HMGB1 levels in conditioned media derived from resting (untreated, 5, 15, 30 min) and activated (50 μM ADP, 5, 15, 30 min; 5 μg/ml CRP, 5, 15, 30 min) platelets were also measured by ELISA. In addition, surface expression of P-selectin (CD62P) on platelets was investigated by staining with a CD62P-specific monoclonal antibody and flow cytometry. *Error bars*, S.E.

tion ($p < 0.002$); sodium azide, 49.0 ± 11.0 *versus* $9.0 \pm 7.7\%$ inhibition ($p < 0.007$; Fig. 5*B*) and apoptotic cardiac fibroblasts (staurosporine, 57.4 ± 9.1 *versus* $9.6 \pm 7.8\%$ inhibition ($p < 0.003$); sodium azide, 53.0 ± 8.9 *versus* $6.7 \pm 6.7\%$ inhibition ($p \leq 0.002$; Fig. 5*D*) nearly completely. Blocking TLR-4 on MSC was followed by similar effects when CM derived from ADP-activated platelets was used prior to evaluating MSC recruitment to CM of apoptotic cardiac myocytes (staurosporine, 48.0 ± 6.8 *versus* $10.1 \pm 6.7\%$ inhibition ($p < 0.003$); sodium azide, 47.1 ± 8.8 *versus* $8.5 \pm 6.4\%$ inhibition ($p < 0.004$; Fig. 5*C*) and apoptotic cardiac fibroblasts (staurosporine, 49.2 ± 9.5 *versus* $10.7 \pm 6.6\%$ inhibition ($p < 0.005$); sodium azide, 49.4 ± 7.6 *versus* $11.9 \pm 7.7\%$ inhibition ($p < 0.004$; Fig. 5*E*).
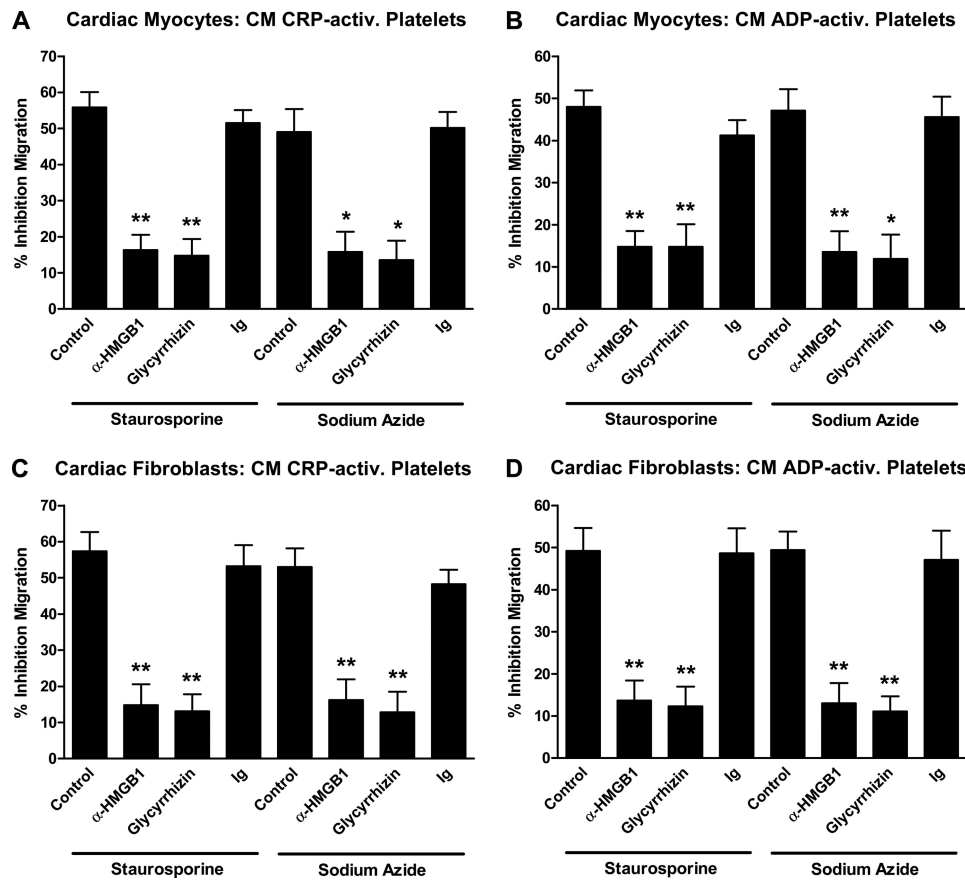
FIGURE 4. **Role of HMGB1 in platelet-mediated inhibition of MSC migration to apoptotic cardiac myocytes and fibroblasts.** MSC were preincubated with conditioned media derived from CRP-activated (5 μg/ml CRP, 30 min) (*A* and *C*) or ADP-activated (50 μM ADP, 30 min) platelets (*B* and *D*) with or without the addition of 10 μg/ml anti-HMGB1 neutralizing antibody, 10 μg/ml glycyrrhizin, or control antibody before migration toward conditioned media of staurosporine-treated or sodium azide-treated cardiac myocytes (*A* and *B*) or cardiac fibroblasts (*C* and *D*) was assessed in transwell migration experiments. The number of migrating MSC was determined after 12 h. Data (mean ± S.E. (*error bars*) for $n \geq 3$) are presented as percentage inhibition calculated from the number of migrating MSC that have not been preincubated with conditioned media derived from activated platelets. Statistical significance (*, $p < 0.02$; **, $p < 0.01$) is indicated.

To validate the role of TLR-4 in platelet-mediated inhibition of MSC recruitment to apoptotic cardiac cells, we performed gene knockdown of TLR-4 in MSC by transfecting the cells with TLR-4 siRNA. To assure the effectiveness of TLR-4 knockdown, Western blot analysis was performed 48 h after transfection to determine TLR-4 protein expression. Following treatment with TLR-4 siRNA, TLR-4 protein expression was significantly ($p < 0.05$) reduced compared with control siRNA-treated and untreated cells (Fig. 5*F*). Next, transfected or non-transfected MSC were incubated with CM derived from activated platelets and subsequently tested for their migration toward apoptotic cardiac myocytes (Fig. 5*G*) or cardiac fibroblasts (Fig. 5*H*). TLR-4 knockdown in MSC was followed by a significantly reversed inhibitory effect of CM derived from CRP-activated (staurosporine, 54.3 ± 7.3 *versus* 32.7 ± 7.0% inhibition ($p < 0.021$); sodium azide, 47.9 ± 11.4 *versus* 29.0 ± 7.5% inhibition ($p < 0.075$)) or ADP-activated platelets (staurosporine, 46.4 ± 6.3 *versus* 26.8 ± 7.2% inhibition ($p < 0.024$); sodium azide, 46.3 ± 7.5 *versus* 28.6 ± 7.9% inhibition ($p < 0.049$)) on MSC migration toward CM of apoptotic cardiac myocytes (Fig. 5*G*). When CM derived from apoptotic cardiac fibroblasts was used as a target for MSC recruitment, similar results were obtained (CM CRP-activated platelets: staurospo-

rine, 57.7 ± 9.0 *versus* 33.9 ± 8.5% inhibition ($p < 0.03$); sodium azide, 53.8 ± 9.0 *versus* 31.6 ± 8.3% inhibition ($p < 0.035$); CM ADP-activated platelets: staurosporine, 48.6 ± 8.6 *versus* 29.0 ± 8.0% inhibition ($p < 0.044$); sodium azide, 50.2 ± 8.3 *versus* 29.6 ± 8.4% inhibition ($p < 0.04$)) (Fig. 5*H*).

Migration of MSC to Apoptotic Cardiac Cells Is Mediated by HGF—We have previously shown that apoptosis but not necrosis in tissue cells results in up-regulation of HGF, which contributes as a major factor to recruitment of MSC (19, 45). To test and confirm the biological relevance of HGF for the cell death-dependent recruitment of MSC toward apoptotic cardiac cells, we performed immunofluorescence staining of intracellular HGF in vital, apoptotic, and necrotic cardiac myocytes coupled with confocal laser-scanning microscopy (Fig. 6*A*). Consistent with our previous observations, HGF could only be detected in apoptotic and not in necrotic or vital cardiac myocytes. To further substantiate HGF expression and release by apoptotic cardiac cells, we determined HGF protein levels in CM of vital, apoptotic (treated with staurosporine or sodium azide), and necrotic (treated with H_2O_2 or ethanol) cardiac myocytes and fibroblasts and detected significant protein levels only in CM of the apoptotic cells (Fig. 6*B*). In migration experiments, the addition of a neutralizing antibody to HGF signifi-
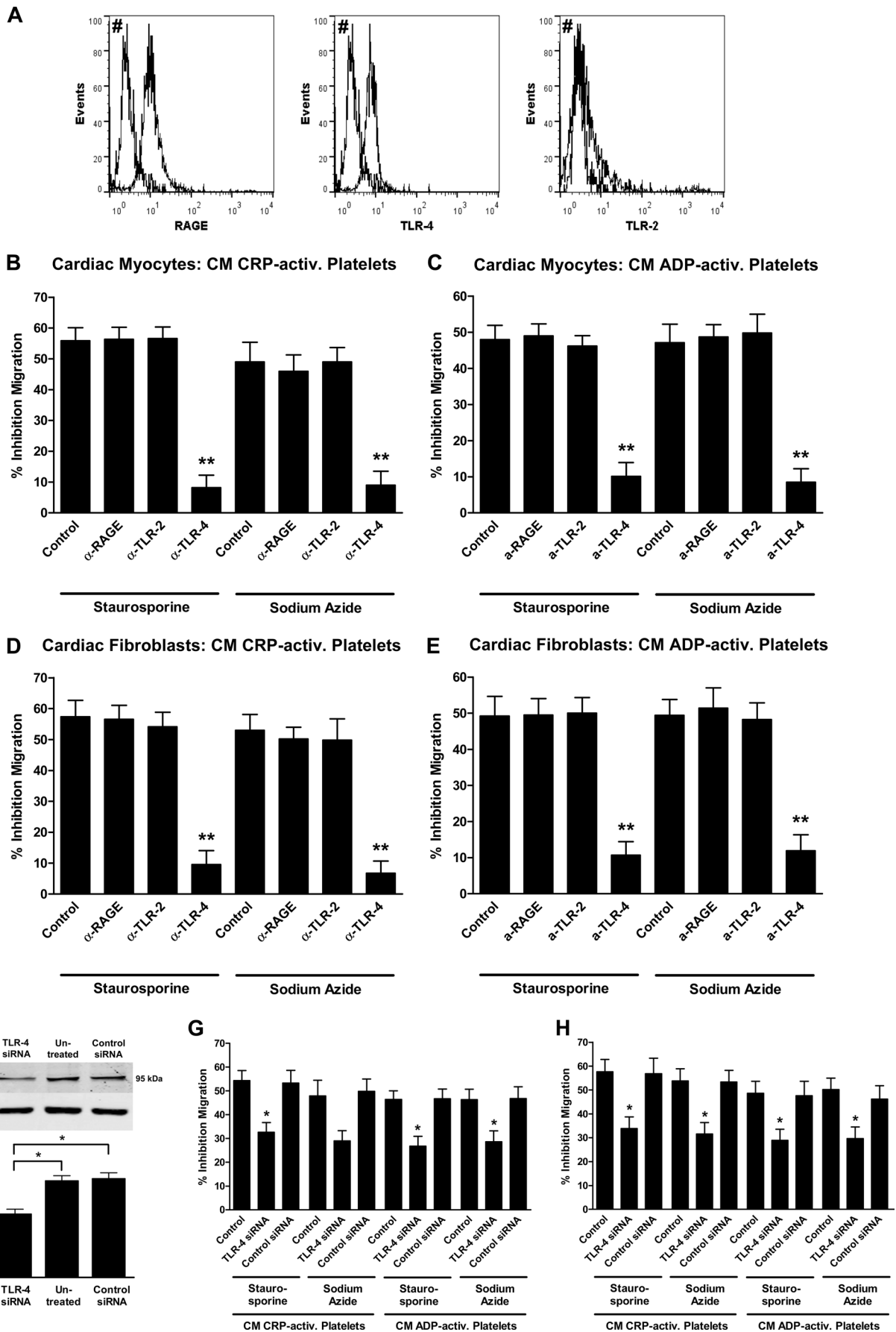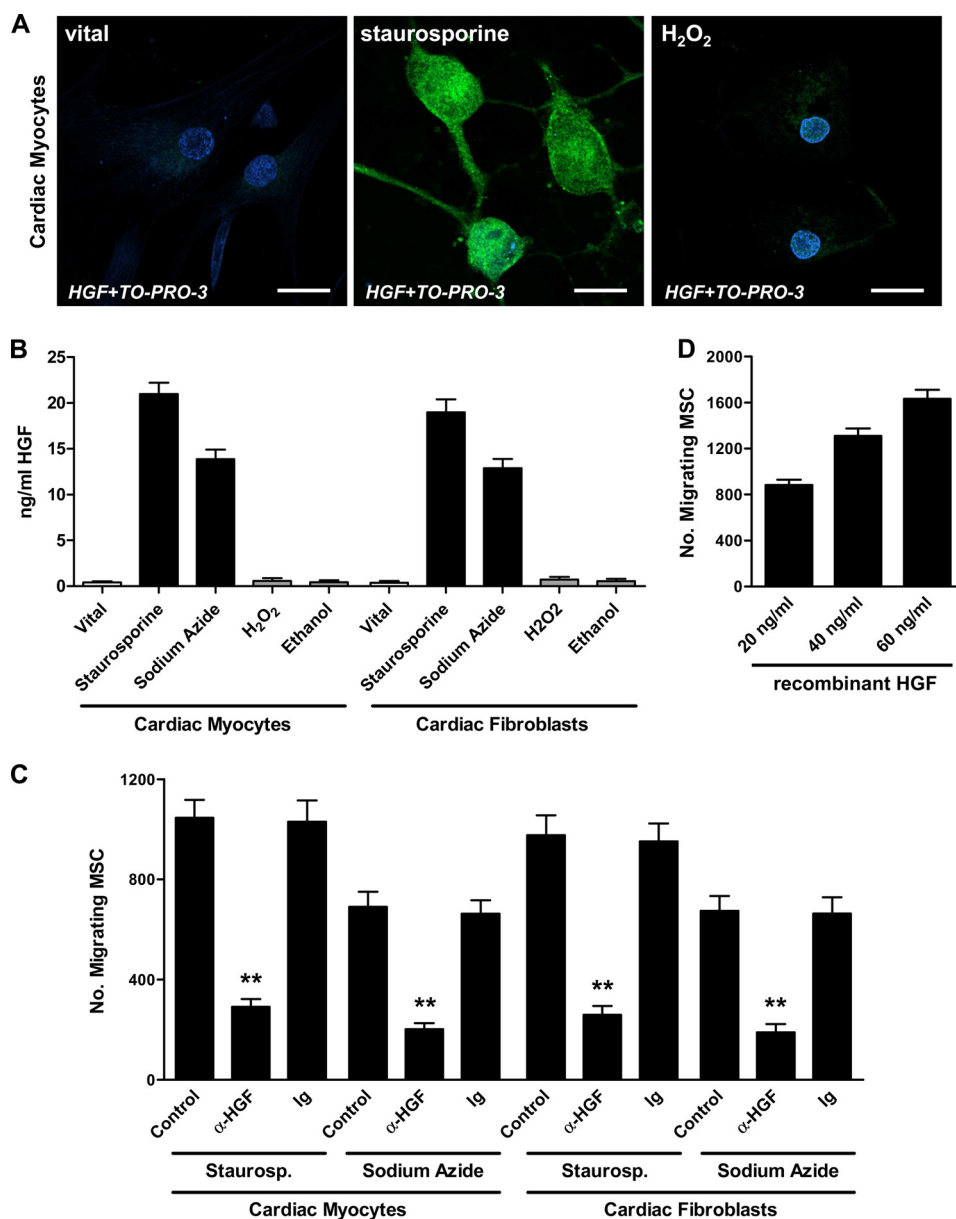
FIGURE 6. **Role of HGF in apoptosis-induced migration of MSC.** *A*, expression of intracellular HGF in vital (untreated), apoptotic (300 nM staurosporine, 3 h), and necrotic (40 μM H_2O_2, 3 h) cardiac myocytes was evaluated by immunofluorescence staining and confocal laser-scanning microscopy. An HGF-specific polyclonal antibody and an Alexa Fluor 488-tagged antibody (*green*) were used. *Blue*, nuclear staining with TO-PRO-3 iodide. Representative images of two independent experiments are shown. *Scale bar*, 20 μm. *B*, HGF levels in conditioned media derived from vital (untreated), apoptotic (300 nM staurosporine, 3 h; 10 mM sodium azide, 3 h), or necrotic (40 μM H_2O_2, 3 h; 25% ethanol, 1 h) cardiac myocytes or cardiac fibroblasts were measured by ELISA. Conditioned media derived from staurosporine-treated or sodium azide-treated cardiac myocytes or cardiac fibroblasts in the presence or absence of 1 μg/ml anti-HGF neutralizing antibody or control antibody (*C*) or graded doses of recombinant HGF (*D*) served as targets in transwell migration experiments. Data are presented as mean ± S.E. (*error bars*) ($n \geq 3$). Statistical significance (**, $p \leq 0.002$) is indicated.

FIGURE 5. **Contribution of individual HMGB1 receptors to the platelet-mediated inhibition of MSC migration to apoptotic cardiac myocytes and fibroblasts.** *A*, expression of HMGB1 receptors RAGE, TLR-2, and TLR-4 on MSC was determined by flow cytometry after staining with specific antibodies. Histograms were set according to negative control stainings (#). MSC were preincubated with conditioned media derived from CRP-activated (5 μg/ml CRP, 30 min) (*B* and *D*) or ADP-activated (50 μM ADP, 30 min) platelets (*C* and *E*) in the presence or absence of neutralizing antibodies to RAGE, TLR-2, and TLR-4 before migration toward conditioned media of staurosporine-treated or sodium azide-treated cardiac myocytes (*B* and *C*) or cardiac fibroblasts (*D* and *E*) was assessed in transwell migration experiments. *F*, knockdown of TLR-4 expression in MSC was carried out through transfection of MSC with siRNA against TLR-4 and validated by Western blot analysis, detecting TLR-4 at 95 kDa. A non-targeting sequence and untreated MSC served as controls for transfection; an actin polyclonal antibody served as loading control. Statistical significance (*, $p < 0.05$) of densitometric analysis of TLR-4 bands (normalized to actin) is indicated. To evaluate the migratory potential of transfected or non-transfected MSC, cells were incubated with conditioned media derived from CRP-activated (5 μg/ml CRP, 30 min) or ADP-activated (50 μM ADP, 30 min) platelets before migration toward conditioned media of staurosporine-treated or sodium azide-treated cardiac myocytes (*G*) or cardiac fibroblasts (*H*) was assessed in transwell migration experiments. Cell migration data (mean ± S.E. (*error bars*) for $n \geq 3$) are presented as percentage inhibition calculated from the number of migrating MSC that have not been preincubated with conditioned media derived from activated platelets. Statistical significance (*, $p < 0.05$; **, $p < 0.007$) of cell migration data is indicated.
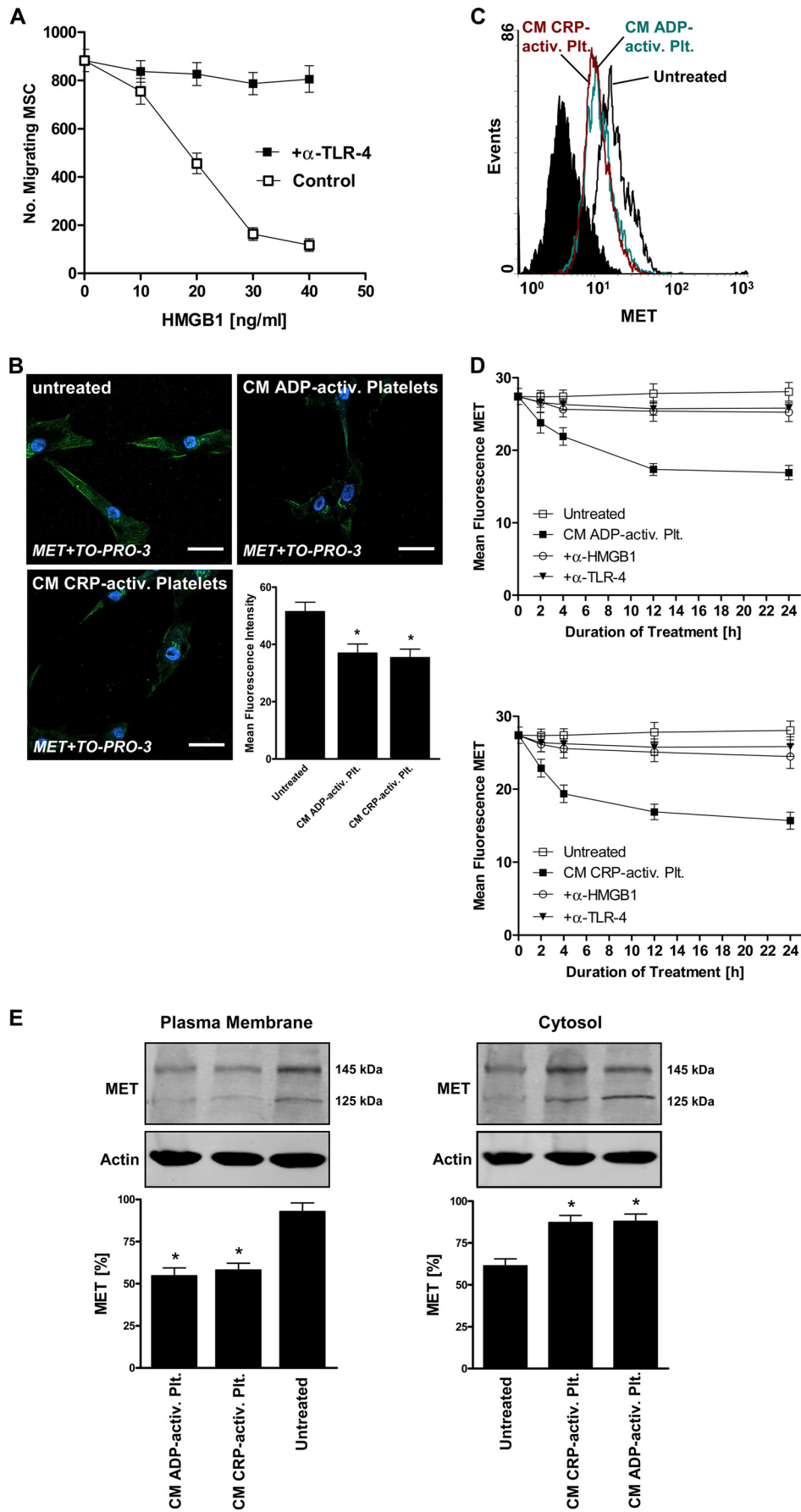
cantly inhibited recruitment of MSC toward CM derived from apoptotic cardiac myocytes (staurosporine, $72.2 \pm 5.4\%$ inhibition ($p < 0.001$); sodium azide, $70.7 \pm 5.9\%$ inhibition ($p < 0.002$)) and apoptotic cardiac fibroblasts (staurosporine, $73.5 \pm 6.4\%$ inhibition ($p < 0.002$); sodium azide, $71.9 \pm 8.4\%$ inhibition ($p \leq 0.002$)) (Fig. 6C). Moreover, recombinant HGF dose-dependently induced MSC migration (Fig. 6D).

Activated Platelets Impair HGF-driven Migration of MSC through HMGB1/TLR-4-mediated Down-regulation of HGF Receptor MET—Having identified HGF as a major factor that drives recruitment of MSC to apoptotic cardiac cells and having detected platelet-derived HMGB1 as a pivotal factor that impairs this cell death-dependent migratory response via TLR-4, we asked ourselves whether recombinant HMGB1 inhibits MSC migration to recombinant HGF in a TLR-4-dependent fashion as well. Indeed, MSC preincubation with recombinant HMGB1 dose-dependently inhibited migration of MSC toward recombinant HGF (20 ng/ml HGF; Fig. 7A). Again, the inhibitory effect of HMGB1 on HGF-mediated MSC migration could be reversed in the presence of a neutralizing antibody against TLR-4.

Because these observations were very suggestive, we finally investigated surface expression of the HGF receptor MET on MSC. As evaluated by immunofluorescence confocal laser-scanning microscopy, untreated MSC were strongly positive for MET, whereas a 24-h incubation of MSC with CM derived from ADP-activated ($28.1 \pm 12.2\%$ inhibition; $p < 0.019$) or CRP-activated platelets ($31.3 \pm 11.5\%$ inhibition; $p < 0.011$) significantly reduced MET surface expression (Fig. 7B; representative results of three experiments). Down-regulation of MET on MSC in response to CM derived from activated platelets could also be detected by flow cytometry (Fig. 7C; representative results of three experiments). Further, time-dependent kinetic curves of mean fluorescence intensity of MET evaluated by flow cytometry were plotted over a 24-h observation period (Fig. 7D). Expression of MET on MSC was significantly reduced during incubation with CM derived from CRP-activated (4 h, $29.3 \pm 6.2\%$ inhibition ($p < 0.033$); 24 h, $44.0 \pm 5.9\%$ inhibition ($p < 0.02$)) or ADP-activated platelets (12 h, $37.6 \pm 4.1\%$ inhibition ($p < 0.022$); 24 h, $39.7 \pm 4.9\%$ inhibition ($p < 0.021$)). In the presence of neutralizing antibodies to HMGB1 as well as TLR-4, no or very little MET down-regulation was observed during incubation with CM of activated platelets, indicating that activated platelets down-regulate surface expression of MET on MSC via HMGB1/TLR-4. Moreover, fractionation of MSC and Western blot analysis performed on plasma membrane and cytosol fractions revealed strong MET expression in the plasma membrane of untreated MSC and, upon treatment with CM derived from CRP-activated as well as ADP-activated platelets, a significant ($p < 0.05$) decrease of MET protein abundance in plasma membrane fractions and increase in the respective cytosol fractions, indicating internalization of the receptor (Fig. 7E).

DISCUSSION

The major findings of the present study are that (i) MSC migrate toward apoptotic but not necrotic or vital cardiac myocytes and fibroblasts in an HGF-dependent fashion, (ii) activated platelets inhibit this cell death-dependent migratory response, and (iii) activated platelets release the alarmin HMGB1, which induces internalization of HGF receptor MET through TLR-4 on MSC, thereby impairing HGF-driven recruitment of MSC to apoptotic cardiac cells. We thus identified a novel mechanism by which platelets control migration of MSC toward damaged cardiac myocytes and fibroblasts. Our findings imply that interactions between platelets and MSC may play a critical role in regulating tissue repair mechanisms after myocardial injury.

The current treatment strategy of acute myocardial infarction relies on rapid reperfusion and secondary prevention therapy that aims to counteract the progression of cardiac dysfunction (46). However, a large number of patients are refractory to standard therapy. Although stem cell-based therapy for the treatment of myocardial ischemia and infarction is still in its preliminary phase, it has the potential to beneficially affect ventricular remodeling and significantly improve heart function (12, 17, 18, 47). To increase the efficacy of stem cell therapy, there is an urgent need to identify critical molecular mechanisms that either promote or impair recruitment of stem cells to the injured myocardium and to therapeutically target specific mechanisms based on these findings.

Platelets have been shown to play a critical role in regulating recruitment of adult stem cells, including MSC, CD34-positive progenitor cells, smooth muscle cell progenitors, and endothelial progenitors, to vascular and tissue lesions (26, 48–51). For instance, platelets are capable of promoting MSC migration, which was dependent on basic fibroblast growth factor (49). Here, we show that activated platelets release HMGB1, a nuclear protein that acts as a danger signal in extracellular space (32), and thereby substantially impair recruitment of MSC to apoptotic cardiac myocytes and fibroblasts.

Platelets are known to express HMGB1 and, upon activation, transport the protein toward the cell surface (34). In patients with disseminated intravascular coagulation associated with

FIGURE 7. **Effect of platelet activation on expression of HGF receptor MET on MSC.** *A*, MSC were preincubated with graded doses of recombinant HMGB1 (10–40 ng/ml) for 24 h and then tested for migration toward recombinant HGF (20 ng/ml) in the presence or absence of a neutralizing TLR-4 antibody. The number of migrating MSC was determined after 12 h. *B*, surface expression of HGF receptor MET on untreated MSC and MSC incubated with conditioned media derived from ADP- or CRP-activated platelets for 24 h was evaluated by immunofluorescence staining and confocal laser-scanning microscopy. A MET-specific polyclonal antibody and an Alexa Fluor 488-tagged antibody (*green*) were used. *Blue*, nuclear staining with TO-PRO-3 iodide. Shown is quantification of MET expression by mean fluorescence intensity. Statistical significance (*, $p < 0.02$) is indicated. Representative images of three independent experiments are shown. *Scale bar*, 40 μm. *C* and *D*, expression of MET on untreated MSC and MSC incubated with conditioned media derived from ADP- or CRP-activated platelets (2, 4, 12, and 24 h) in the presence or absence of neutralizing antibodies to HMGB1 or TLR-4 was also determined by flow cytometry and quantified by mean fluorescence intensity. *E*, down-regulation of MET on MSC was further studied by fractionation of untreated MSC and MSC incubated with conditioned media derived from ADP- or CRP-activated platelets for 12 h into plasma membrane and cytosolic components, and subsequent Western blot analysis was performed on the distinct fractions, detecting MET at 145 and 125 kDa. Data are presented as mean $\pm$ S.E. (*error bars*) ($n \geq 3$). Statistical significance (*, $p < 0.05$) of densitometric analysis of MET bands (normalized to actin) is indicated.

hematologic malignancy, serum levels of HMGB1 significantly correlated with platelet activation markers (52). HMGB1 typically mediates recruitment of innate immune cells and stimulates inflammatory responses, such as release of proinflammatory cytokines through binding to receptors RAGE, TLR-2, and TLR-4 (32). Importantly, MSC express HMGB1 receptors (41, 42), implying that MSC are a putative target for platelet-derived HMGB1. Enhanced (53) as well as reduced (42) migratory activity of MSC has been reported as a result of TLR ligation. In our study, platelet-derived HMGB1 inhibited the cell death-dependent migratory response of MSC via TLR-4. Interestingly, increased ventricular performance could be observed after intracoronary injection of MSC derived from TLR-4-knock-out mice into an isolated infarcted rat heart, whereupon Wang *et al.* concluded that activation of TLR-4 on MSC impairs their cardioprotective activity after myocardial infarction by a STAT3-inhibitory mechanism (54). In another study, ligation of TLR-4 has been shown to result in the development of proinflammatory activities of MSC, such as activation of T-lymphocytes and increased production of proinflammatory mediators (55). These findings indicate that ligation of platelet-derived HMGB1 to TLR-4 expressed on MSC may counteract MSC-mediated cardioprotection and provide favorable conditions for inflammation. Moreover, the mechanism identified in this study may contribute to the common limitation of the only short lived beneficial effects of MSC-based therapy for the treatment of myocardial ischemia and infarction. As a consequence, blocking TLR-4 on MSC or gene knockdown might improve the efficacy of MSC-based therapy due to an improved infiltration into the damaged target tissue.

Clinical grade MSC are expanded *in vitro* preferentially with animal serum-free media containing platelet-rich plasma (PRP) due to lower risk of infectious complications and host immune reactions (56). Incubation of MSC with PRP significantly enhanced MSC migration capacities compared with incubation with fetal calf serum (57). However, PRP also contains significant amounts of HMGB1, which may be relevant for the cell death-dependent migratory response of clinical grade MSC cultured in media supplemented with PRP.

In the present study, only apoptotic and not necrotic cardiac myocytes and fibroblasts produced HGF and induced migration of MSC via HGF receptor MET. Thus, the type of cell death appears to control whether recruitment of MSC, a prerequisite for their cardioprotective effects, takes place or not. Necrosis is usually a result of extreme tissue damage and induces inflammatory responses, whereas apoptosis is typically associated with immunological tolerance, although the microenvironment may modulate this outcome (58). HGF and MSC have immunosuppressive (24, 59), antiapoptotic (10, 22), and cardioprotective (7, 25) effects. HGF-mediated recruitment of MSC to apoptotic cardiac cells therefore appears to be a critical mechanism for MSC-mediated repair and regeneration of the injured myocardium. Here, we provide evidence that activated platelets directly interfere with this tissue repair mechanism through HMGB1/TLR-4-dependent down-regulation of HGF receptor MET on MSC.

In conclusion, we have identified a novel mechanism by which platelets, upon activation, substantially impair migration of MSC to apoptotic cardiac myocytes and fibroblasts. Our data may be of particular relevance for further investigations regarding the cross-talk between platelets and MSC and its influence on myocardial repair and regeneration. Such new insights will hopefully help us to develop better stem cell-based therapeutics for the injured heart.

REFERENCES

1. Ertl, G., and Frantz, S. (2005) Healing after myocardial infarction. *Cardiovasc. Res.* **66,** 22–32
2. Frangogiannis, N. G., Smith, C. W., and Entman, M. L. (2002) The inflammatory response in myocardial infarction. *Cardiovasc. Res.* **53,** 31–47
3. Pfeffer, M. A., and Braunwald, E. (1990) Ventricular remodeling after myocardial infarction. Experimental observations and clinical implications. *Circulation* **81,** 1161–1172
4. Dominici, M., Le Blanc, K., Mueller, I., Slaper-Cortenbach, I., Marini, F., Krause, D., Deans, R., Keating, A., Prockop, D., and Horwitz, E. (2006) Minimal criteria for defining multipotent mesenchymal stromal cells. The International Society for Cellular Therapy position statement. *Cytotherapy* **8,** 315–317
5. Pittenger, M. F., Mackay, A. M., Beck, S. C., Jaiswal, R. K., Douglas, R., Mosca, J. D., Moorman, M. A., Simonetti, D. W., Craig, S., and Marshak, D. R. (1999) Multilineage potential of adult human mesenchymal stem cells. *Science* **284,** 143–147
6. Wen, Z., Zheng, S., Zhou, C., Wang, J., and Wang, T. (2011) Repair mechanisms of bone marrow mesenchymal stem cells in myocardial infarction. *J. Cell Mol. Med.* **15,** 1032–1043
7. Wollert, K. C., and Drexler, H. (2005) Mesenchymal stem cells for myocardial infarction: promises and pitfalls. *Circulation* **112,** 151–153
8. Makino, S., Fukuda, K., Miyoshi, S., Konishi, F., Kodama, H., Pan, J., Sano, M., Takahashi, T., Hori, S., Abe, H., Hata, J., Umezawa, A., and Ogawa, S. (1999) Cardiomyocytes can be generated from marrow stromal cells *in vitro*. *J. Clin. Invest.* **103,** 697–705
9. Lee, C. H., Shah, B., Moioli, E. K., and Mao, J. J. (2010) CTGF directs fibroblast differentiation from human mesenchymal stem/stromal cells and defines connective tissue healing in a rodent injury model. *J. Clin. Invest.* **120,** 3340–3349
10. Li, J. H., Zhang, N., and Wang, J. A. (2008) Improved anti-apoptotic and anti-remodeling potency of bone marrow mesenchymal stem cells by anoxic pre-conditioning in diabetic cardiomyopathy. *J. Endocrinol. Invest.* **31,** 103–110
11. Mias, C., Lairez, O., Trouche, E., Roncalli, J., Calise, D., Seguelas, M. H., Ordener, C., Piercecchi-Marti, M. D., Auge, N., Salvayre, A. N., Bourin, P., Parini, A., and Cussac, D. (2009) Mesenchymal stem cells promote matrix metalloproteinase secretion by cardiac fibroblasts and reduce cardiac ventricular fibrosis after myocardial infarction. *Stem Cells* **27,** 2734–2743
12. Gnecchi, M., He, H., Liang, O. D., Melo, L. G., Morello, F., Mu, H., Noiseux, N., Zhang, L., Pratt, R. E., Ingwall, J. S., and Dzau, V. J. (2005) Paracrine action accounts for marked protection of ischemic heart by Akt-modified mesenchymal stem cells. *Nat. Med.* **11,** 367–368
13. Gnecchi, M., Zhang, Z., Ni, A., and Dzau, V. J. (2008) Paracrine mechanisms in adult stem cell signaling and therapy. *Circ. Res.* **103,** 1204–1219
14. Amado, L. C., Saliaris, A. P., Schuleri, K. H., St John, M., Xie, J. S., Cattaneo, S., Durand, D. J., Fitton, T., Kuang, J. Q., Stewart, G., Lehrke, S., Baumgartner, W. W., Martin, B. J., Heldman, A. W., and Hare, J. M. (2005) Cardiac repair with intramyocardial injection of allogeneic mesenchymal stem cells after myocardial infarction. *Proc. Natl. Acad. Sci. U.S.A.* **102,** 11474–11479
15. Chen, S. L., Fang, W. W., Ye, F., Liu, Y. H., Qian, J., Shan, S. J., Zhang, J. J., Chunhua, R. Z., Liao, L. M., Lin, S., and Sun, J. P. (2004) Effect on left ventricular function of intracoronary transplantation of autologous bone

marrow mesenchymal stem cell in patients with acute myocardial infarction. *Am. J. Cardiol.* **94,** 92–95

16. Nagaya, N., Fujii, T., Iwase, T., Ohgushi, H., Itoh, T., Uematsu, M., Yamagishi, M., Mori, H., Kangawa, K., and Kitamura, S. (2004) Intravenous administration of mesenchymal stem cells improves cardiac function in rats with acute myocardial infarction through angiogenesis and myogenesis. *Am. J. Physiol. Heart Circ. Physiol.* **287,** H2670–H2676

17. Assmus, B., Honold, J., Schächinger, V., Britten, M. B., Fischer-Rasokat, U., Lehmann, R., Teupe, C., Pistorius, K., Martin, H., Abolmaali, N. D., Tonn, T., Dimmeler, S., and Zeiher, A. M. (2006) Transcoronary transplantation of progenitor cells after myocardial infarction. *N. Engl. J. Med.* **355,** 1222–1232

18. Wollert, K. C., Meyer, G. P., Lotz, J., Ringes-Lichtenberg, S., Lippolt, P., Breidenbach, C., Fichtner, S., Korte, T., Hornig, B., Messinger, D., Arseniev, L., Hertenstein, B., Ganser, A., and Drexler, H. (2004) Intracoronary autologous bone-marrow cell transfer after myocardial infarction: the BOOST randomised controlled clinical trial. *Lancet* **364,** 141–148

19. Vogel, S., Trapp, T., Börger, V., Peters, C., Lakbir, D., Dilloo, D., and Sorg, R. V. (2010) Hepatocyte growth factor-mediated attraction of mesenchymal stem cells for apoptotic neuronal and cardiomyocytic cells. *Cell Mol. Life Sci.* **67,** 295–303

20. Ono, K., Matsumori, A., Shioi, T., Furukawa, Y., and Sasayama, S. (1997) Enhanced expression of hepatocyte growth factor/c-Met by myocardial ischemia and reperfusion in a rat model. *Circulation* **95,** 2552–2558

21. Zhu, Y., Hojo, Y., Ikeda, U., and Shimada, K. (2000) Production of hepatocyte growth factor during acute myocardial infarction. *Heart* **83,** 450–455

22. Xiao, G. H., Jeffers, M., Bellacosa, A., Mitsuuchi, Y., Vande Woude, G. F., and Testa, J. R. (2001) Anti-apoptotic signaling by hepatocyte growth factor/Met via the phosphatidylinositol 3-kinase/Akt and mitogen-activated protein kinase pathways. *Proc. Natl. Acad. Sci. U.S.A.* **98,** 247–252

23. Aoki, M., Morishita, R., Taniyama, Y., Kida, I., Moriguchi, A., Matsumoto, K., Nakamura, T., Kaneda, Y., Higaki, J., and Ogihara, T. (2000) Angiogenesis induced by hepatocyte growth factor in non-infarcted myocardium and infarcted myocardium: up-regulation of essential transcription factor for angiogenesis, ets. *Gene Ther.* **7,** 417–427

24. Okunishi, K., Dohi, M., Nakagome, K., Tanaka, R., Mizuno, S., Matsumoto, K., Miyazaki, J., Nakamura, T., and Yamamoto, K. (2005) A novel role of hepatocyte growth factor as an immune regulator through suppressing dendritic cell function. *J. Immunol.* **175,** 4745–4753

25. Nakamura, T., Mizuno, S., Matsumoto, K., Sawa, Y., and Matsuda, H. (2000) Myocardial protection from ischemia/reperfusion injury by endogenous and exogenous HGF. *J. Clin. Invest.* **106,** 1511–1519

26. Gawaz, M., and Vogel, S. (2013) Platelets in tissue repair: control of apoptosis and interactions with regenerative cells. *Blood* **122,** 2550–2554

27. Borst, O., Münzer, P., Gatidis, S., Schmidt, E. M., Schönberger, T., Schmid, E., Towhid, S. T., Stellos, K., Seizer, P., May, A. E., Lang, F., and Gawaz, M. (2012) The inflammatory chemokine CXC motif ligand 16 triggers platelet activation and adhesion via CXC motif receptor 6-dependent phosphatidylinositide 3-kinase/Akt signaling. *Circ. Res.* **111,** 1297–1307

28. Fitzgerald, D. J., Roy, L., Catella, F., and FitzGerald, G. A. (1986) Platelet activation in unstable coronary disease. *N. Engl. J. Med.* **315,** 983–989

29. Gawaz, M., Langer, H., and May, A. E. (2005) Platelets in inflammation and atherogenesis. *J. Clin. Invest.* **115,** 3378–3384

30. Trip, M. D., Cats, V. M., van Capelle, F. J., and Vreeken, J. (1990) Platelet hyperreactivity and prognosis in survivors of myocardial infarction. *N. Engl. J. Med.* **322,** 1549–1554

31. Willerson, J. T., Golino, P., Eidt, J., Campbell, W. B., and Buja, L. M. (1989) Specific platelet mediators and unstable coronary artery lesions. Experimental evidence and potential clinical implications. *Circulation* **80,** 198–205

32. Andersson, U., and Tracey, K. J. (2011) HMGB1 is a therapeutic target for sterile inflammation and infection. *Annu. Rev. Immunol.* **29,** 139–162

33. Erlandsson Harris, H., and Andersson, U. (2004) Mini-review: The nuclear protein HMGB1 as a proinflammatory mediator. *Eur. J. Immunol.* **34,** 1503–1512

34. Rouhiainen, A., Imai, S., Rauvala, H., and Parkkinen, J. (2000) Occurrence of amphoterin (HMG1) as an endogenous protein of human platelets that

is exported to the cell surface upon platelet activation. *Thromb. Haemost.* **84,** 1087–1094

35. Kohno, T., Anzai, T., Naito, K., Miyasho, T., Okamoto, M., Yokota, H., Yamada, S., Maekawa, Y., Takahashi, T., Yoshikawa, T., Ishizaka, A., and Ogawa, S. (2009) Role of high-mobility group box 1 protein in post-infarction healing process and left ventricular remodelling. *Cardiovasc. Res.* **81,** 565–573

36. Andrassy, M., Volz, H. C., Igwe, J. C., Funke, B., Eichberger, S. N., Kaya, Z., Buss, S., Autschbach, F., Pleger, S. T., Lukic, I. K., Bea, F., Hardt, S. E., Humpert, P. M., Bianchi, M. E., Mairbäurl, H., Nawroth, P. P., Remppis, A., Katus, H. A., and Bierhaus, A. (2008) High-mobility group box-1 in ischemia-reperfusion injury of the heart. *Circulation* **117,** 3216–3226

37. Kitahara, T., Takeishi, Y., Harada, M., Niizeki, T., Suzuki, S., Sasaki, T., Ishino, M., Bilim, O., Nakajima, O., and Kubota, I. (2008) High-mobility group box 1 restores cardiac function after myocardial infarction in transgenic mice. *Cardiovasc. Res.* **80,** 40–46

38. Oozawa, S., Mori, S., Kanke, T., Takahashi, H., Liu, K., Tomono, Y., Asanuma, M., Miyazaki, I., Nishibori, M., and Sano, S. (2008) Effects of HMGB1 on ischemia-reperfusion injury in the rat heart. *Circ. J.* **72,** 1178–1184

39. Park, J. S., Gamboni-Robertson, F., He, Q., Svetkauskaite, D., Kim, J. Y., Strassheim, D., Sohn, J. W., Yamada, S., Maruyama, I., Banerjee, A., Ishizaka, A., and Abraham, E. (2006) High mobility group box 1 protein interacts with multiple Toll-like receptors. *Am. J. Physiol. Cell Physiol.* **290,** C917–C924

40. Park, J. S., Svetkauskaite, D., He, Q., Kim, J. Y., Strassheim, D., Ishizaka, A., and Abraham, E. (2004) Involvement of Toll-like receptors 2 and 4 in cellular activation by high mobility group box 1 protein. *J. Biol. Chem.* **279,** 7370–7377

41. Kume, S., Kato, S., Yamagishi, S., Inagaki, Y., Ueda, S., Arima, N., Okawa, T., Kojiro, M., and Nagata, K. (2005) Advanced glycation end-products attenuate human mesenchymal stem cells and prevent cognate differentiation into adipose tissue, cartilage, and bone. *J. Bone Miner. Res.* **20,** 1647–1658

42. Pevsner-Fischer, M., Morad, V., Cohen-Sfady, M., Rousso-Noori, L., Zanin-Zhorov, A., Cohen, S., Cohen, I. R., and Zipori, D. (2007) Toll-like receptors and their ligands control mesenchymal stem cell functions. *Blood* **109,** 1422–1432

43. Gawaz, M., Neumann, F. J., Dickfeld, T., Koch, W., Laugwitz, K. L., Adelsberger, H., Langenbrink, K., Page, S., Neumeier, D., Schömig, A., and Brand, K. (1998) Activated platelets induce monocyte chemotactic protein-1 secretion and surface expression of intercellular adhesion molecule-1 on endothelial cells. *Circulation* **98,** 1164–1171

44. Stellos, K., Bigalke, B., Stakos, D., Henkelmann, N., and Gawaz, M. (2010) Platelet-bound P-selectin expression in patients with coronary artery disease. Impact on clinical presentation and myocardial necrosis, and effect of diabetes mellitus and anti-platelet medication. *J. Thromb. Haemost.* **8,** 205–207

45. Vogel, S., Peters, C., Etminan, N., Börger, V., Schimanski, A., Sabel, M. C., and Sorg, R. V. (2013) Migration of mesenchymal stem cells towards glioblastoma cells depends on hepatocyte-growth factor and is enhanced by aminolaevulinic acid-mediated photodynamic treatment. *Biochem. Biophys. Res. Commun.* **431,** 428–432

46. Gerczuk, P. Z., and Kloner, R. A. (2012) An update on cardioprotection: a review of the latest adjunctive therapies to limit myocardial infarction size in clinical trials. *J. Am. Coll. Cardiol.* **59,** 969–978

47. Britten, M. B., Abolmaali, N. D., Assmus, B., Lehmann, R., Honold, J., Schmitt, J., Vogl, T. J., Martin, H., Schächinger, V., Dimmeler, S., and Zeiher, A. M. (2003) Infarct remodeling after intracoronary progenitor cell treatment in patients with acute myocardial infarction (TOPCARE-AMI): mechanistic insights from serial contrast-enhanced magnetic resonance imaging. *Circulation* **108,** 2212–2218

48. Langer, H., May, A. E., Daub, K., Heinzmann, U., Lang, P., Schumm, M., Vestweber, D., Massberg, S., Schönberger, T., Pfisterer, I., Hatzopoulos, A. K., and Gawaz, M. (2006) Adherent platelets recruit and induce differentiation of murine embryonic endothelial progenitor cells to mature endothelial cells in vitro. *Circ. Res.* **98,** e2–e10

49. Langer, H. F., Stellos, K., Steingen, C., Froihofer, A., Schönberger, T.,

ASBMB

Krämer, B., Bigalke, B., May, A. E., Seizer, P., Müller, I., Gieseke, F., Siegel-Axel, D., Meuth, S. G., Schmidt, A., Wendel, H. P., Bloch, W., and Gawaz, M. (2009) Platelet derived bFGF mediates vascular integrative mechanisms of mesenchymal stem cells in vitro. *J. Mol. Cell Cardiol.* **47,** 315–325

50. Massberg, S., Konrad, I., Schürzinger, K., Lorenz, M., Schneider, S., Zohlnhoefer, D., Hoppe, K., Schiemann, M., Kennerknecht, E., Sauer, S., Schulz, C., Kerstan, S., Rudelius, M., Seidl, S., Sorge, F., Langer, H., Peluso, M., Goyal, P., Vestweber, D., Emambokus, N. R., Busch, D. H., Frampton, J., and Gawaz, M. (2006) Platelets secrete stromal cell-derived factor 1α and recruit bone marrow-derived progenitor cells to arterial thrombi in vivo. *J. Exp. Med.* **203,** 1221–1233

51. Stellos, K., Langer, H., Daub, K., Schoenberger, T., Gauss, A., Geisler, T., Bigalke, B., Mueller, I., Schumm, M., Schaefer, I., Seizer, P., Kraemer, B. F., Siegel-Axel, D., May, A. E., Lindemann, S., and Gawaz, M. (2008) Platelet-derived stromal cell-derived factor-1 regulates adhesion and promotes differentiation of human CD34$^+$ cells to endothelial progenitor cells. *Circulation* **117,** 206–215

52. Nomura, S., Fujita, S., Ozasa, R., Nakanishi, T., Miyaji, M., Mori, S., Ito, T., and Ishii, K. (2011) The correlation between platelet activation markers and HMGB1 in patients with disseminated intravascular coagulation and hematologic malignancy. *Platelets* **22,** 396–397

53. Tomchuck, S. L., Zwezdaryk, K. J., Coffelt, S. B., Waterman, R. S., Danka, E. S., and Scandurro, A. B. (2008) Toll-like receptors on human mesenchymal stem cells drive their migration and immunomodulating responses. *Stem Cells* **26,** 99–107

54. Wang, Y., Abarbanell, A. M., Herrmann, J. L., Weil, B. R., Manukyan, M. C., Poynter, J. A., and Meldrum, D. R. (2010) TLR4 inhibits mesenchymal stem cell (MSC) STAT3 activation and thereby exerts deleterious effects on MSC-mediated cardioprotection. *PLoS One* **5,** e14206

55. Waterman, R. S., Tomchuck, S. L., Henkle, S. L., and Betancourt, A. M. (2010) A new mesenchymal stem cell (MSC) paradigm: polarization into a pro-inflammatory MSC1 or an immunosuppressive MSC2 phenotype. *PLoS One* **5,** e10088

56. Müller, I., Kordowich, S., Holzwarth, C., Spano, C., Isensee, G., Staiber, A., Viebahn, S., Gieseke, F., Langer, H., Gawaz, M. P., Horwitz, E. M., Conte, P., Handgretinger, R., and Dominici, M. (2006) Animal serum-free culture conditions for isolation and expansion of multipotent mesenchymal stromal cells from human BM. *Cytotherapy* **8,** 437–444

57. Murphy, M. B., Blashki, D., Buchanan, R. M., Yazdi, I. K., Ferrari, M., Simmons, P. J., and Tasciotti, E. (2012) Adult and umbilical cord blood-derived platelet-rich plasma for mesenchymal stem cell proliferation, chemotaxis, and cryo-preservation. *Biomaterials* **33,** 5308–5316

58. Chen, G. Y., and Nuñez, G. (2010) Sterile inflammation: sensing and reacting to damage. *Nat. Rev. Immunol.* **10,** 826–837

59. Uccelli, A., Moretta, L., and Pistoia, V. (2008) Mesenchymal stem cells in health and disease. *Nat. Rev. Immunol.* **8,** 726–736